arXiv:1605.03812v1 [cond-mat.supr-con] 12 May 2016

Superconducting Properties of the Non-Centrosymmetric Superconductor Re_6Hf

D. Singh,[1] A. D. Hillier,[2] A. Thamizhavel,[3] and R. P. Singh[1,*]

[1] *Indian Institute of Science Education and Research Bhopal, Bhopal, 462066, India*
[2] *ISIS facility, STFC Rutherford Appleton Laboratory, Harwell Science and Innovation Campus, Oxfordshire, OX11 0QX, UK*
[3] *Department of Condensed Matter Physics and Materials Science, Tata Institute of Fundamental Research, Mumbai 400005, India*

(Dated: May 13, 2016)

The synthesis and detailed characterization of the noncentrosymmetric superconductor Re_6Hf using powder x-ray diffraction (XRD), magnetization, transport and thermodynamic measurements are reported. XRD confirms the crystal structure of Re_6Hf to be cubic noncentrosymmetric α-*Mn* with a lattice parameter a = 9.6850(3)Å. Resistivity, DC and AC magnetization confirms the bulk superconducting transition $T_c^{onset} \sim$ 5.96 K. The lower critical field $H_{C1}(0) \approx 5.6$ mT and upper critical $H_{C2}(0)$ was found to be around 12.2 T which is greater than the Pauli limiting field, indicating unconventional behavior in Re_6Hf and leads to the possibility of triplet pairing. A sharp discontinuity in the specific heat data was observed around T_c indicating bulk superconductivity, and the normalized specific heat jump is $\Delta C_{el}/\gamma_n T_c = 1.53$ which is in close agreement with BCS value. Superconducting electronic specific heat data is fitted reasonably well for an exponential relation with Sommerfeld coefficient (γ) showing a linear relation with magnetic field suggesting that in Re_6Hf dominant pairing channel is s-wave with isotropic superconducting gap parameter without nodes.

INTRODUCTION

In 1957, Bardeen, Cooper and Schrieffer (BCS) explained the origin of superconductivity using concept of Cooper pairs [1]. Cooper pairs are constructed from electrons that have equal and opposite crystal momenta and opposite spin. The pairs are formed via an electron-phonon interaction. Because electrons are fermions, the wavefunction must be antisymmetric with respect to the exchange of the two electrons. The two electron wave function can be made asymmetric by considering the spatial and spin components. If spatial wavefunction is symmetric/anti-symmetric, the spin wavefunction must be anti-symmetric/symmetric. This is termed as spin- singlet state /spin-triplet state. This scenario is only possible if inversion symmetry is present in crystal structure [2, 3].

There has been an intense theoretical and experimental studies on superconducting system lacking spatial inversion symmetry, after the discovery of unconventional superconductivity in noncentrosymmetric heavy fermion compound $CePt_3Si$ [4]. In NCS's absence of center of inversion induces Rashba-type antisymmetric spin orbit coupling (ASOC) due to an asymmetric potential gradient along the crystal axis; this momentum dependent spin structure in consequence lifts the degeneracy of the conduction band electrons at Fermi surface resulting into the possible mixing of spin-singlet and spin-triplet pair states [5–9]. The magnitude of ASOC splitting, actually dictates the extent of mixing of spin singlet and spin-triplet components. The possible mixing of pair states in noncentrosymmetric superconductors may lead to various novel superconducting properties such as upper critical field exceeding Pauli limit, line or point nodes in superconducting gap parameter resulting into nodal excitations in penetration depth, heat capacity and other thermodynamic measurements, time reversal symmetry breaking in superconducting condensate.

Apart from $CePt_3Si$ [4] several other Ce and U-based heavy fermionic NCS's $CeRhSi_3$ [10, 11], $CeIrSi_3$ [12, 13], $CeCoGe_3$ [14], UIr [15], UGe_2 [16] were discovered with applied pressure, but it doesn't resolve the problem as strong electron correlations in this f-electron systems with magnetic quantum criticality hinder the pursuit to realize the effects of ASOC and absence of inversion center on superconductivity. Superconductivity in these systems is expected to be due to non-conventional pairing mechanism, most likely driven by magnetic fluctuations.

Several weakly and strongly correlated non-centrosymmetric superconducting systems e.g. $Li_2(Pd,Pt)_3B$ [17–20], $LaNiC_2$ [21, 22], Re_3W [23], $Mg_{10}Ir_{19}B_{16}$ [24], La *MP*(*M*=Ir, Rh and *P*=P, As) [25], Mo_3Al_2C [26], Ru_7B_3 [27, 28], $Nb_{0.18}Re_{0.82}$ [29, 30], Re_6Zr [31, 33], La_7Ir_3 [32], have been investigated to understand the pairing mechanism and found that only few of them have exhibited unconventional superconducting behavior including triplet pairing [31, 32, 34] and upper critical field close to the Pauli limit [35] others have shown only dominant s-wave characters.

* rpsingh@iiserb.ac.in

In this paper, we present the synthesis, characterization and physical properties of intermetallic binary compound Re_6Hf, exhibiting bulk superconductivity at $T_c^{onset} \sim 5.96$ K. Re_6Hf crystallizes into cubic non-centrosymmetric crystal structure with space group $I\bar{4}3m$. Low temperature magnetic, transport and heat capacity measurements suggest dominant s-wave character with upper critical field higher than the Pauli limiting field, indicating the signature of spin triplet component.

EXPERIMENTAL DETAILS

Polycrystalline sample of Re_6Hf (3g) was synthesized using standard arc melting technique where stoichiometric amount of Hf(4N) and Re(4N) taken in a nominal ratio of 6:1 on a water cooled copper hearth under the flow of high purity argon gas. Both the elements are melted together to make a single button of Re_6Hf, then flipped and remelted several times for the sample homogeneity. The sample formed is hard, silvery grey in color with negligible mass loss.
XRD was carried out in Panalytical diffractometer using Cu K_α radiation (λ= 1.54056 Å) for the characterization of crystal structure and phase purity.

Magnetization and AC susceptibility measurements were performed using Quantum Design Superconducting Quantum Interference Device (SQUID MPMS , Quantum Design) down to a temperature 1.8 K. In magnetization measurement the sample was cooled down to 1.8 K in zero field and then 10 mT field was applied. The measurement was carried out while warming it to 10 K called ZFCW mode whereas for FCC mode sample was cooled down in 10 mT field with data taken simultaneously. Magnetization and AC susceptibility measurements were also done in a temperature range between 1.8 K to 8.0 K under an applied magnetic fields up to 7.0 T.
The heat-capacity measurement was performed by the two tau time-relaxation method using the physical property measurement system (PPMS, Quantum Design, Inc.) in zero and applied magnetic fields up to 7.0 T. The electrical resistivity measurements were performed in PPMS (Quantum Design, Inc.) by using conventional four-probe ac technique at 157 Hz and at excitation current of 10 mA. The measurements was done in zero field from 1.85 K to 300 K to know the resistivity ρ_0 and residual resistivity ratio (RRR).

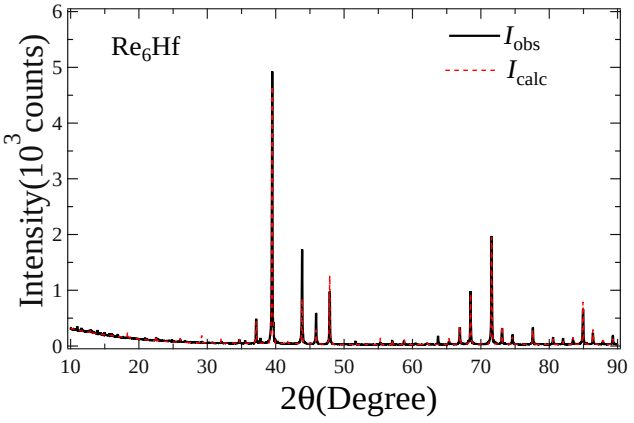

FIG. 1. (color online) Powder XRD pattern for Re_6Hf sample recorded at room temperature using Cu K_α radiation. Rietveld refined calculated pattern for cubic α-Mn (217) noncentrosymmetric structure shown by solid red line.

RESULTS AND DICUSSION

Sample characterization

Polycrystalline sample of Re_6Hf was crushed into a very fine powder for XRD analysis. The powder XRD data collected from sample of Re_6Hf at room temperature shown in Fig.1 and were Rietveld refined by using High Score Plus Software. As evident from the pattern that sample was in single phase with no impurity traces found whatsoever. Crystal structure was confirmed to be cubic noncentrosymmetric α-Mn structure, primitive Bravais lattice $I\bar{4}3m$ (space group 217) with cubic cell parameter a = 9.6850(3)Å. There are two formula units per unit cell. Refined cell parameters and atomic positions is shown in Table I

TABLE I. Crystal structure Lattice and Rietveld refinement parameters obtained from the room temperature powder X-ray Diffraction of Re_6Hf

Structure	Cubic
Space group	$I\bar{4}3m$
Lattice parameters	
a(Å)	9.6850(3)
V_{cell}(Å^3)	908

Atomic Coordinates

Atom	Wyckoff position	x	y	z
Re1	24g	0.106	0.106	0.288
Re2	24g	0.344	0.344	0.031
Hf1	8c	0.315	0.315	0.315
Hf2	2a	0	0	0

Normal and Superconducting State properties

Electrical resistivity

The normal state temperature dependence of the resistivity for Re_6Hf between 1.85 K and 300 K in zero magnetic field is shown in Fig.2(a), where the resistivity increases leisurely with temperature showing poor metallic behavior. The residual resistivity ratio is found to be $\rho(300/\rho(10) = 1.47$, suggesting that the polycrystalline sample is dominated by disorder. This behavior is similar to other Re based α-Mn compounds $Nb_{0.18}Re_{0.82}$ (RRR∼1.3) [29], $Re_{24}Ti_5$ (RRR∼1.3) [36] and Re_6Zr (RRR∼1.10)[31, 33]. An expanded plot of the zero-field ρ(T) data is shown in the inset of Fig.2(a), which shows a superconducting transition with a transition width of ΔT = 0.41 K, with an onset at T_c^{onset} = 5.96 K and zero resistance at T = 5.55 K

The low temperature resistivity data has been fitted using power law

$$\rho = \rho_0 + AT^n \quad (1)$$

from 10 K ≤ T ≤ 50 K, as shown in Fig.2(b) by the solid red line where ρ_0 is the residual resistivity due to crystallographic defects, A is the coefficient associated with the temperature dependence of electric resistivity which is taken as measure of degree of electron-electron correlation.

Using Eq. 1, we found n ∼ 2.2 ± 0.1 with ρ_0 = 106.12 ± 0.02 $\mu\Omega$ cm and A = (2.34 ± 0.01) × 10^{-3} $\mu\Omega$ cmK^2. The higher value of ρ_0 is most likely due to polycrystalline nature of the sample. The value of A is very low indicating a weakly correlated system whereas n is close to 2 suggesting a Fermi-liquid behavior in the normal state low temperature resistivity data.

Magnetization

The superconductivity in Re_6Hf was confirmed by the magnetization data taken in ZFCW and FCC mode as shown in Fig.3. The data was taken in low applied field of 10 mT, shows the onset of strong diamagnetic signal due to superconducting transition at T_c^{onset} = 5.94 K. Superconducting transition was further confirmed by AC susceptibility (Fig.4) measurement.

Fig.5(a) shows the low field (0-30 mT) magnetization M(H) curves for Re_6Hf taken at several temperatures. Lower critical field $H_{C1}(T)$ is defined as the field deviating from the linear line for the initial slope. The H_{C1} is 5.2 mT at T = 1.8 K and decreases monotonically with increase in temperature to 1.0 mT at T = 5.5 K. The temperature variation of $H_{C1}(T)$ is shown in Fig.5(b), as expected $H_{C1}(T)$ is varying as a function of T^2 in accordance with Ginzburg-Landau (GL) theory

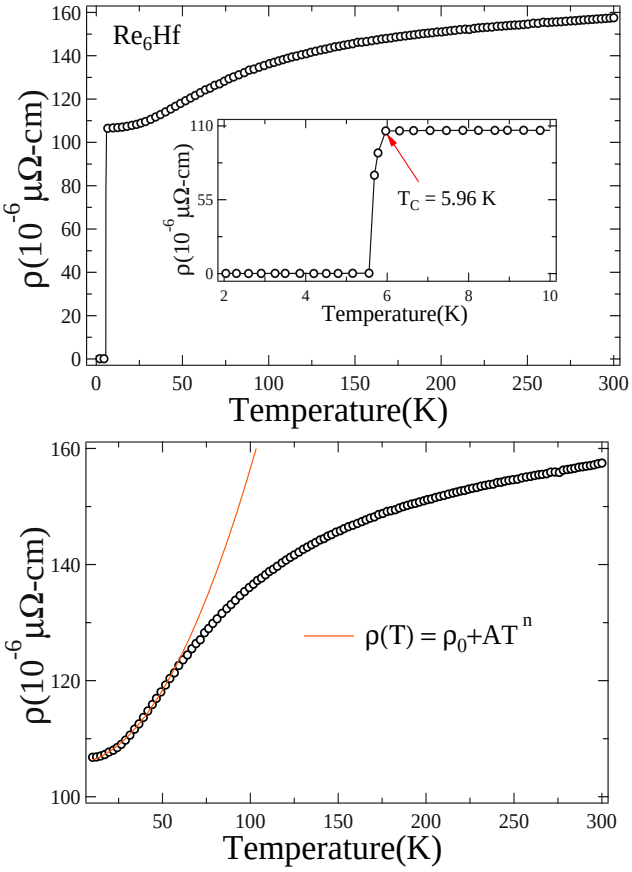

FIG. 2. (color online)(a) Temperature dependence of resistivity for Re_6Hf shown over the range 1.85 K ≤ T ≤ 300 K. Inset shows superconducting transition at T_c^{onset} = 5.96 K. (b) Power law fitting over the temperature range 10 K ≤ T ≤ 50 K gives n = 2.2 ± 0.1 indicating Fermi-liquid behavior at low temperature

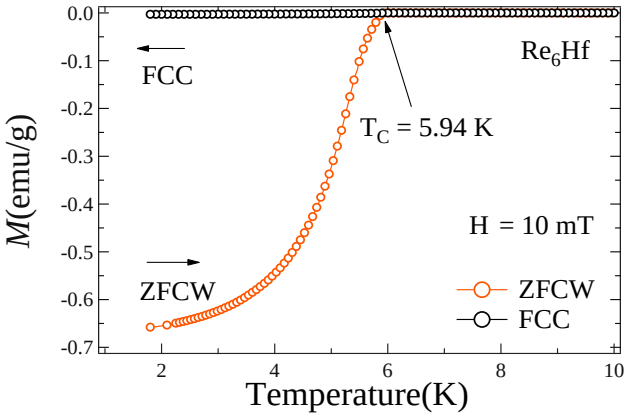

FIG. 3. (color online) Temperature dependence of the magnetic moment, collected via zero-field cooled warming (ZFCW) and field cooled cooling (FCC) methods under an applied field of 10 mT.

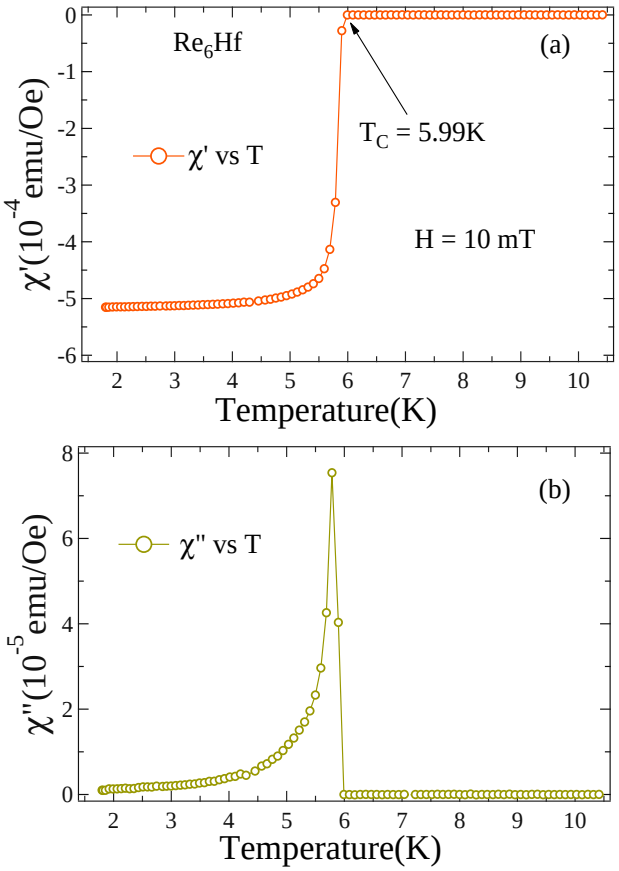

FIG. 4. (color online) Temperature dependence of AC susceptibility for Re_6Hf.

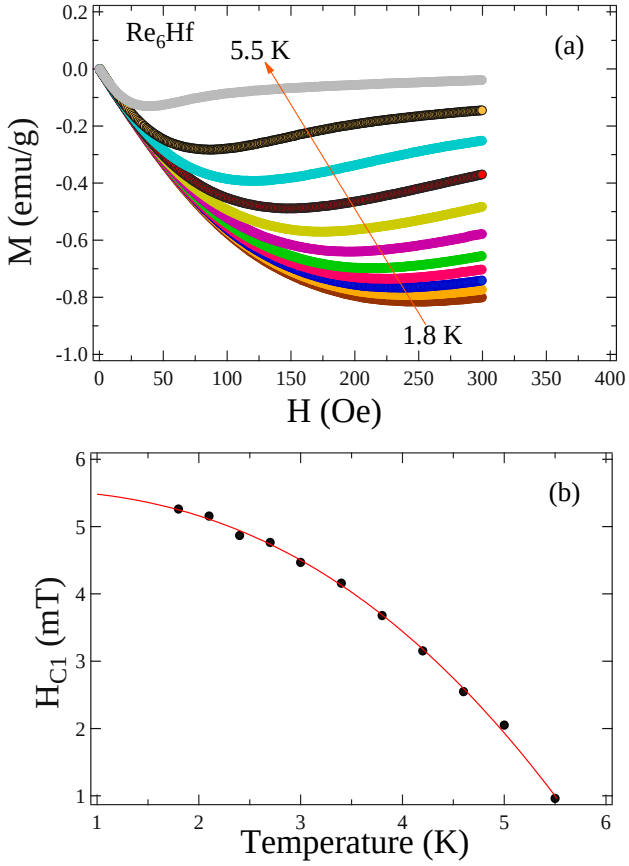

FIG. 5. (color online) (a) Isothermal magnetization for Re_6Hf at various temperatures (b) Fitting using Eq. 2 gives $H_{C1}(0) \sim 5.6$ mT

$$H_{C1}(T) = H_{C1}(0)\left(1 - \left(\frac{T}{T_c}\right)^2\right) \tag{2}$$

Lower critical field $H_{C1}(0)$ was estimated to be 5.6 ± 0.5 mT by fitting the relation given in Eq. 2 in the data given in Fig.5(b).

A magnetization curve at 1.8 K in high applied magnetic field range ($\pm$ 7 T) is showed in Fig.6. As evident from the graph that Re_6Hf exhibits a conventional type - II superconductivity. H_{irr} was estimated from magnetization curve, is 1.80 T at 1.8 K, therefore for fields $H > H_{irr}$ unpinning of vortices starts taking place.

Specific heat

The specific heat $C(T)$ measurement for Re_6Hf in zero field in the temperature range 1.85 K $\leq$ T $\leq$ 10 K is shown in Fig.7(a). The superconducting transition in specific heat data is manifested by a sharp jump in $C(T)$ at T_c = 5.96 K, confirming bulk superconductivity in Re_6Hf. The field dependence of the specific heat is shown in Fig.7(b). The specific heat jump near T_c moves to lower temperature and the size of the jump ΔC becomes smaller with increasing magnetic field. The normal state low temperature specific heat can be extracted easily with the relation

$$\frac{C}{T} = \gamma_n + \beta_3 T^2 + \beta_5 T^4 \tag{3}$$

where the extrapolation of normal state behavior below T_c to the $T \to 0$ limit, allow the determination of normal state Sommerfeld coefficient γ_n, debye constant β_3 and anharmonic contribution β_5 to lattice heat capacity. By fitting the above relation (3) between 36 K $\leq T^2 \leq$ 100 K, shown by red line in Fig.8(a) we obtained γ_n=27.2 $\pm$ 0.1 mJ/moleK^2, β_3=0.28 $\pm$ 0.05 mJ/moleK^4 and β_5=0.0014 $\pm$ 0.0003 μJ/moleK^6.

The Debye temperature θ_D is related to β_3 coefficient through formula

$$\theta_D = \left(\frac{12\pi^4 RN}{5\beta}\right)^{\frac{1}{3}} \tag{4}$$

where R is the molar gas constant(=8.314 $Jmole^{-1}K^{-1}$). Using N (= 14) the number of atoms per

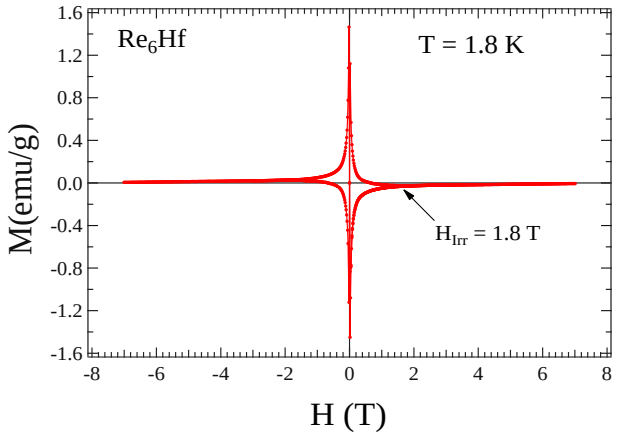

FIG. 6. (color online) Magnetization vrs magnetic field variation at T = 1.8 K. The magnetization is irreversible below a field HIrr = 1.8 T.

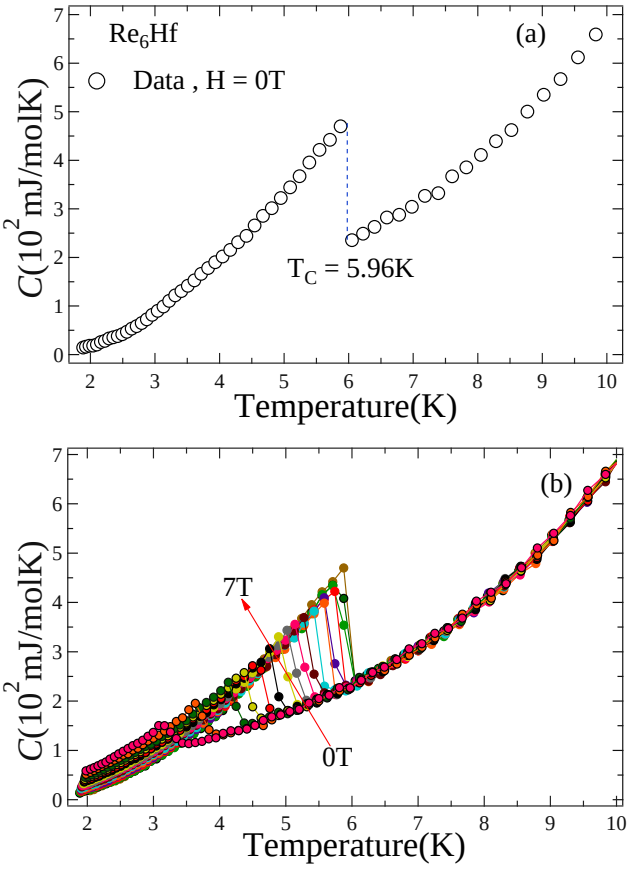

FIG. 7. (color online) (a) Temperature dependence of specific heat in zero-field showing superconducting transition at T_c = 5.96 K (b) Field dependence of the specific heat data, showing the suppression of T_c with increasing field.

unit cell, gives $\theta_D = 365$ K. For non-interacting particles the Sommerfeld coefficient is proportional to density of states $D_C(E_F)$ at the Fermi level which is calculated to be 11.53 $\frac{states}{eV f.u}$ from the relation given by

$$\gamma_n = \left(\frac{\pi^2 k_B^2}{5}\right) D_C(E_f) \tag{5}$$

where $k_B \approx 1.38 \times 10^{-23}$ J K^{-1}.
This calculated density of states $D_C(E_f)$ and the effective mass m^* of quasi-particles contains the influence of many body electron-phonon interaction and is related to bare band-structure density of states $D_{band}(E_f)$ and m^*_{band} according to

$$D_C(E_f) = D_{band}(E_f)(1 + \lambda_{e-ph}) \tag{6}$$

$$m^* = m^*_{band}(1 + \lambda_{e-ph}) \tag{7}$$

where λ_{e-ph} is the dimensionless electron phonon coupling constant. Electron-phonon coupling constant which gives the strength of attractive interaction between electron-phonon can be calculated using θ_D and T_C given in McMillan theory [37] by

$$\lambda_{e-ph} = \frac{1.04 + \mu^* ln(\theta_D/1.45T_c)}{(1 - 0.62\mu^*) ln(\theta_D/1.45T_c) - 1.04} \tag{8}$$

where μ^* is the repulsive screened coulomb parameter, typically given by $\mu^* = 0.13$ for many intermetallic superconductors. Using T_c= 5.96 K (from our specific heat measurement) we obtained $\lambda_{e-ph} = 0.63$. This value is comparable to other fully gapped non-centrosymmetric superconductors such as 0.6 for $Re_{24}Ti_5$ [36], 0.5 for $Nb_{0.18}Re_{0.82}$ [29], Re_6Zr [33], $SrAuSi_3$ [38] suggesting that Re_6Hf is a moderately coupled superconductor. Using the value of λ_{e-ph}, we calculated $D_{band}(E_f)$ to be equal to 7.04 $\frac{states}{eV f.u}$, also by taking $m^*_{band} = m_e$ the effective mass for the quasi-particles comes out be 1.63 m_e. The mean free path l can be estimated using the relation

$$l = 3\pi^2 \left(\frac{\hbar}{e^2 \rho_0}\right) \left(\frac{\hbar}{m^* v_f}\right)^2 \tag{9}$$

where the Fermi velocity v_f is given by

$$v_f = \frac{\pi^2 \hbar^3 D_C(E_f)}{m^{*2} V_{f.u}} \tag{10}$$

where $V_{f.u} = \frac{V_{cell}}{2}$ is the volume per formula unit. Using $D_C(E_f)$ value 11.53 $\frac{states}{eV f.u}$ we calculated $v_f = 8.27 \times 10^5$ cm/s which gives mean free path l = 8.5 Å

The electronic contribution to specific heat in superconducting state $C_{el}(T)$ for Re_6Hf is shown in Fig.8(b) and can be calculated by subtracting the phononic contribution from the measured data $C(T)$

$$C_{el}(T) = C(T) - \beta^3 T^3 + \beta^5 T^5 \tag{11}$$

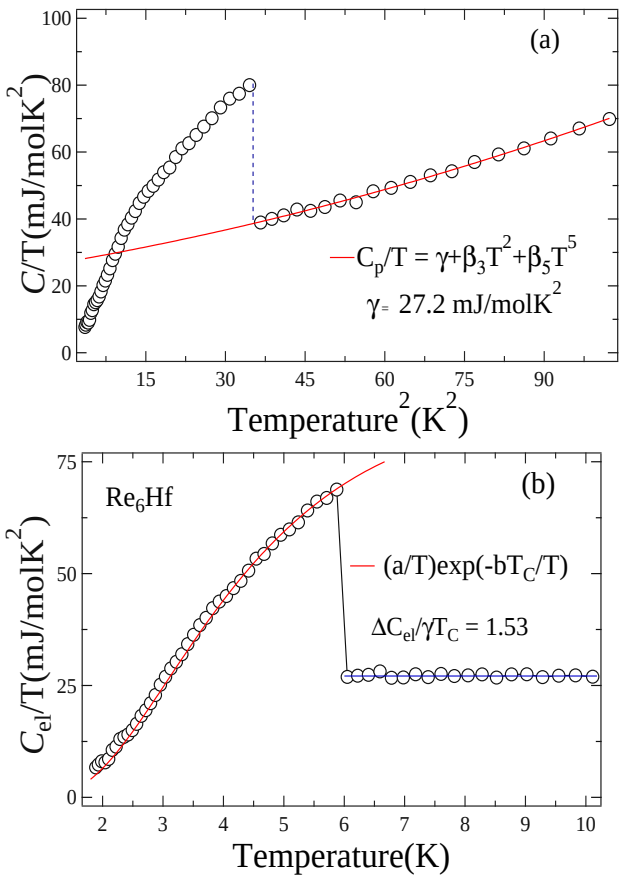

FIG. 8. (color online) (a) C/T vs T^2 for 36 K $\leq \mathrm{T}^2 \leq$ 100 K in zero field well described by the equation $\frac{C}{T} = \gamma_n + \beta_3 T^2 + \beta_5 T^4$ (b) Solid red curve in $\mathrm{C}_{el}/\mathrm{T}$ versus T data shows exponential fitting for b = α = 1.75 which is close the BCS value is α = 1.764.

The magnitude of specific heat jump $\frac{\Delta C_{el}}{T_c}$ at T_c in $\mathrm{C}_{el}/\mathrm{T}$ data is 41.55 mJ/moleK^2 . This gives the normalized specific heat jump $\frac{\Delta C_{el}}{\gamma_n T_c}$ = 1.53 for γ_n =27.2 mJ/moleK^2 which is slightly higher than the BCS value of $\frac{\Delta C_{el}}{\gamma_n T_c}$ = 1.43 in the weak coupling limit.

The temperature dependence of specific data in the superconducting state can best be described by an exponential function given by $\mathrm{C}_{el}/\mathrm{T} = \mathrm{aexp}\left(\frac{-bT_c}{T}\right)$ where b = $\Delta(0)/\mathrm{k}_B\mathrm{T}_c$ for fully gaped s - wave superconductor. As shown in Fig.8(b) we have reasonably good agreement with the above function to our experimental data $\mathrm{C}_{el}/\mathrm{T}$ for b=α = 1.75, which is close to value for a BCS superconductor b = $\Delta(0)/\mathrm{k}_B\mathrm{T}_c$ = 1.764. Therefore the above analysis suggests that for $\mathrm{Re}_6\mathrm{Hf}$ can simply accounted for a BCS type fully gaped superconductor.

The fully gaped s-wave superconductivity in $\mathrm{Re}_6\mathrm{Hf}$ can also be confirmed by the magnetic field dependence of the Sommerfeld coefficient $\gamma(H)$. The Sommerfeld coefficient is proportional to the quasiparticle density of states, hence as we apply more field, the vortex density increases due to an increase in the number of field induced

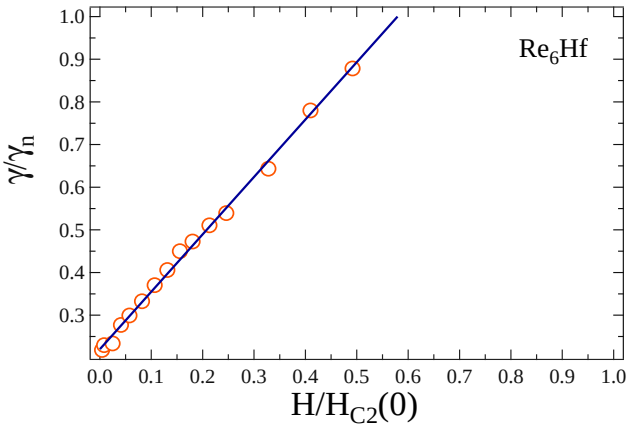

FIG. 9. (color online) γ and H was plotted versus each other after normalizing it by γ_n(=27.2 mJ/molK^2) and $\mathrm{H}_{C2}(0)$(=12.2 T). Solid red curve in γ/γ_n versus $\mathrm{H}/\mathrm{H}_{C2}(0)$ shows the linear relation indicating s - wave superconductivity in $\mathrm{Re}_6\mathrm{Hf}$

vortices which in turn enhances the quasiparticle density of states. This gives rise to linear relation between γ and H i.e., $\gamma(\mathrm{H}) \propto \mathrm{H}$ for a nodeless and isotropic s- wave superconductor [38–40]. For a superconductor with nodes in gap Volovik predicted a non -linear relation given by $\gamma(\mathrm{H}) \propto \mathrm{H}^{\frac{1}{2}}$ [41]

Field dependence of γ is shown in Fig.9 where Sommerfeld coefficient γ was calculated by fitting the relation (12) in $\mathrm{C}_{el}/\mathrm{T}$ versus T data for various fields and extrapolating it to T = 0 K [38]

$$\frac{C_{el}}{T} = \gamma + \frac{A}{T} exp\left(\frac{-bT_c}{T}\right) \tag{12}$$

here we can clearly observe a linear relation between γ(H) and H confirming the s - wave superconductivity in $\mathrm{Re}_6\mathrm{Hf}$ which we have already seen by the exponential signature in at low temperature specific heat measurement.

The condensation energy U (0) can be calculated using γ and $\alpha(= \Delta(0)/k_B T_c$ from the relation

$$U(0) = \frac{1}{2}\Delta^2(0) D_{band}(E_f) = \frac{3\gamma_n \Delta^2(0)}{4\pi^2 k_B^2} \tag{13}$$

which gives U (0) = 225.4 mJ/mole. The magnitude of electron - electron correlation can be given by Kadowaki-Woods ratio which is given by $\mathrm{K}_w = \frac{A}{\gamma_n^2}$, where A is the coefficient of the quadratic temperature dependent resistivity term, whereas γ_n Sommerfeld coefficient . In heavy fermionic systems where electron- electron correlation is significant Kadowaki- Woods ratio K_w approaches 1×10^{-5} $\mu\Omega$cm mJ^{-2}mole^{-2}K^2 [42–44]. For A=0.0023 $\mu\Omega$ cm K^2 and γ_n=27.2 mJ/mole K^2, we found K_w= 0.31×10^{-5} $\mu\Omega$cm mJ^{-2}mole^{-2}K^2 which is smaller than strongly correlated systems indicating that $\mathrm{Re}_6\mathrm{Hf}$ is a weakly correlated system.

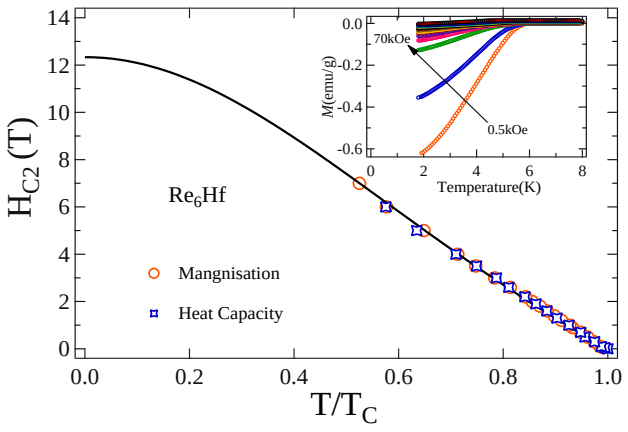

FIG. 10. (color online) (a) Determination of the upper critical field via magnetization and heat capacity measurements.The solid lines are Ginzburg Landau (Eq. 14) fits. Inset shows the *M(T)* curves for various applied magnetic field

Isothermal magnetization curves are measured in magnetic fields upto 7.0 T to calculate the upper critical field $H_{C2}(0)$ as showed in inset of Fig.10. The transition temperature was taken as the onset of diamagnetic signal in magnetization measurement. As the field is increased T_C shifts to lower temperature with superconducting transition becoming broader. $H_{C2}(T)$ was seen to be vary as linearly when plotted against reduced temperature(T/T_c) as displayed in Fig. 10, and can be fitted using Ginzburg-Landau(GL) formula to calculate $H_{C2}(0)$

$$H_{C2}(T) = H_{C2}(0)\frac{(1-t^2)}{(1+t^2)} \tag{14}$$

where t=T/T_c. Our experimental data fits fairly well with equation (14) yielding the upper critical field $H_{C2}(0)$ to be around 12.2 ± 0.1 T. Similar linear behavior of $H_{C2}(T)$ was noted when calculated from specific heat measurements $C(T)$ as shown by blue data points in Fig. 10, when fitted with GL formula gives $H_{C2}(0) \approx 12.2$ T

$H_{C2}(0)$ can be used to estimate the Ginzburg Landau coherence length ξ_{GL} from the relation [45]

$$H_{C2}(0) = \frac{\Phi_0}{2\pi\xi_{GL}^2} \tag{15}$$

where and Φ_0 (=2.07 × 10^{-15} Tm^2) is the magnetic flux quantum. Using $H_{C2}(0)$ = 12.2 T we calculated $\xi_{GL}(0) \approx 52$ Å, mean free path l which is calculated from normal state specific heat data was 8.5 Å is much lower than $\xi_{GL}(0)$ indicating the dirty limit superconductivity in Re_6Hf.

In a type-II superconductor the Cooper pair breaking due to applied magnetic field is attributed to two types of mechanisms Orbital and Pauli paramagnetic limiting field effect. In orbital pair breaking field-induced kinetic energy of Cooper pair exceeds the superconducting condensation energy whereas in Pauli paramagnetic limiting it is energetically favorable for the electron spins to align with magnetic field, thus breaking the Cooper pairs. For BCS superconductors the orbital limit of upper critical field $H_{C2}^{orbital}(0)$ is given by using the WHH expression [46, 47]

$$H_{C2}^{orbital}(0) = -\alpha T_c \left.\frac{-dH_{C2}(T)}{dT}\right|_{T=T_c} \tag{16}$$

where α is the purity factor given by 0.693 for dirty limit superconductors and 0.73 for clean limit superconductors. Initial slope $\left.\frac{-dH_{C2}(T)}{dT}\right|_{T=T_c}$ to be 2.36 T/K from H_{C2}-T phase diagram obtained earlier which gives us the orbital limiting upper critical field $H_{C2}^{orbital}(0)$ in dirty limit 9.77 T. The Pauli limiting field within the BCS theory is given by $H_{C2}^{p}(0)$= 1.86 T_c[48, 49], which for T_c = 5.96 K gives $H_{C2}^{p}(0) \approx$ 11.10 T. The Maki parameter [50] α_M is a measure relative strengths of the orbital and Pauli- limiting values of H_{C2} and is given by

$$\alpha_M = \sqrt{2}H_{C2}^{orb}(0)/H_{C2}^{p}(0) \tag{17}$$

from above relation we obtain α_M = 1.24 .The sizable value of Maki parameter obtained from this expression is an indication that effect of Pauli limiting field is non-negligible [30, 31].

The Ginzburg Landau penetration depth $\lambda_{GL}(0)$ can be obtained from the $H_{C1}(0)$ and $\xi_{GL}(0)$ using the relation [51]

$$H_{C1}(0) = \left(\frac{\Phi_0}{4\pi\lambda_{GL}^2(0)}\right) ln\left(\frac{\lambda_{GL}(0)}{\xi_{GL}(0)}\right) \tag{18}$$

For $H_{C1}(0) \approx 5.6$ mT and $\xi_{GL}(0)$ = 52 Å, we obtain $\lambda_{GL}(0) \approx$ 3538Å The Ginzburg Landau parameter is given by the relation

$$k_{GL} = \frac{\lambda_{GL}(0)}{\xi_{GL}(0)} \tag{19}$$

For $\xi_{GL}(0)$ = 52 Å and $\lambda_{GL}(0)$ = 3538 Å gives $k_{GL} \approx$ 68. This value of $k_{GL} \gg \frac{1}{\sqrt{2}}$ indicating that Re_6Hf is a strong type - II superconductor as already seen from magnetization curve in Fig. 6. Thermodynamic critical field H_C is be obtained from k_{GL} , $H_{C1}(0)$ and $H_{C2}(0)$ using the relation [51]

$$H_{C1}(0)H_{C2}(0) = H_C^2 lnk_{GL} \tag{20}$$

yielding H_C around 126.7 mT.

The Ginzburg number G_i which is basically the ratio of thermal energy K_BT (with upper limit of T is T_c) to condensation energy associated with coherence volume

measure the sensitivity of vortex system against thermal fluctuations is obtained by the from the relation [52, 53]

$$G_i = \frac{1}{2}\left(\frac{k_B\mu_0\tau T_c}{4\pi\xi^3(0)H_{C2}(0)}\right)^2 \quad (21)$$

where τ is anisotropy parameter which is 1 for cubic Re_6Hf. For ξ_0 = 52 Å, $H_C(0)$ = 126.7 mT and T_c= 5.96 K we got G_i= 6.65 × 10^{-2}. As it was already noticed from magnetization curve that melting of vortices starts at field H > H_{irr}(=1.8 T) which is much smaller than upper critical field at 1.8 K H_{C2}(1.8 K)= 10.16 T. This behavior usually found in high temperature superconductors where melting of vortices attributed to thermal fluctuations and very rare in low T_c superconductors. G_i which is found to be of the order same as high T_c superconductors, suggests that thermal fluctuations may be playing important role in unpinning of vortices.

TABLE II. Normal and superconducting properties of Re_6Hf

Atomic Coordinates	unit	value
T_c	K	5.96
ρ_0	$\mu\Omega$cm	106.12
A	$\mu\Omega$cmK^{-2}	0.0023
$H_{C1}(0)$	mT	5.6
$H_{C2}(0)$	T	12.2
$H_C(0)$	mT	126.7
$H_{C2}^{orbital}(0)$	T	9.8
$H_{C2}^{P}(0)$	T	11.1
ξ_{GL}	Å	52
λ_{GL}	Å	3538
k_{GL}		68.0
l	Å	8.5
γ	mJmol^{-1}K^{-2}	27.2
β	mJmol^{-1}K^{-4}	0.28
θ_D	K	365
λ_{ep}		0.63
$D_C(E_f)$	states/ev f.u	11.53
$\Delta C_{el}/\gamma_n T_C$		1.53
$\Delta/k_B T_C$		1.75

CONCLUSION

Single phase polycrystalline sample of Re_6Hf was prepared by arc- melting technique, which crystallizes into non-centrosymmetric α-*Mn* (217) structure with lattice parameter a = 9.6850(3) Å. Transport, magnetization and thermodynamic measurements reveals that Re_6Hf is a weakly correlated type-II superconductor with bulk transition at $T_c \approx$ 5.96 K. Above transition temperature T_C, resistivity measurement shows poor metallic behavior whereas magnetization measurement showed weak paramagnetism. Mean free path calculated l (=8.5 Å) is much smaller than coherence length ξ (= 52 Å) confirms dirty limit superconductivity in Re_6Hf. Low temperature specific heat measurement in superconducting regime indicates that Re_6Hf is a moderately coupled superconductor λ_{e-ph} = 0.63 with normalized specific heat jump $\frac{\Delta C_{el}}{\gamma_n T_c}$ = 1.53. Computed value of upper critical field H_{C2} is greater than Pauli limiting field indicates that there may be spin triplet component in superconducting condensate, however specific heat data in superconducting state fits perfectly well with thermally activated behavior manifested by exponential relation $C_{es} \propto \exp\left(\frac{-bT_c}{T}\right)$ indicating that Re_6Hf is a s-wave superconductor. BCS type superconductivity in Re_6Hf was further confirmed by field dependence of Sommerfeld coefficient $\gamma(H)$ where it varies linearly with H suggesting that electronic states near the Fermi surface are fully gaped. Similar type of behavior observed in Re_6Zr [31] by μSR spectroscopy. Our initial μSR measurements suggest the presence of triplet component which is coherent with current result.

ACKNOWLEDGMENTS

R. P. S. acknowledges Science and Engineering Research Board, Government of India for the Ramanujan Fellowship.

[1] J. Bardeen, L. N. Cooper, and J. R. Schrieffer, Phys. Rev.108, 1175 (1957).
[2] P. W. Anderson, J. Phys. Chem. Solids 11, 26 (1959).
[3] P. W. Anderson, Phys. Rev. B 30, 4000 (1984).
[4] E. Bauer, G. Hilscher, H. Michor, Ch. Paul, E. W. Scheidt, A. Gribanov, Yu. Seropegin, H. Noël, M. Sigrist, and P. Rogl, Phys. Rev. Lett. 92, 027003 (2004).
[5] V. M. Édelshtein, Sov.Phys. JETP 68, 1244 (1989).
[6] L. P. Gor'kov, E. I. Rashba, Phys. Rev. Lett. 87, 037004 (2001).
[7] K. V. Samokhin, E. S. Zijlstra, and S. K. Bose, Phys. Rev. B 69, 094514 (2004).
[8] P. A. Frigeri, D. F. Agterberg, A. Koga, and M. Sigrist, Phys. Rev. Lett. 92, 097001 (2004).
[9] S. Fujimoto, J. Phys. Soc. Jpn. 76, 051008 (2007).
[10] N. Kimura, K. Ito, K. Saitoh, Y. Umeda, H. Aoki, and T. Terashima, Phys. Rev. Lett. 95, 247004 (2005).
[11] N. Kimura, K. Ito, H. Aoki, S. Uji, and T. Terashima, Phys. Rev.Lett. 98, 197001 (2007).
[12] I. Sugitani, Y. Okuda, H. Shishido, T. Yamada, A. Thamizhavel: E. Yamamoto, T. D. Matsuda, Y. Haga, T. Takeuchi, R. Settai, and Y. Ōnuki, J. Phys. Soc. Jpn. 75, 043703 (2006).

[13] R. Settai, Y. Miyauchi, T. Takeuchi, F. Lévy, I. Sheikin, and Y. Ōnuki, J. Phys. Soc. Jpn. 77, 073705 (2008).

[14] R. Settai, I. Sugitani, Y. Okuda, A. Thamizhavel, M. Nakashima, Y. Ōnuki, and H. Harima, J. Magn. Mater. 310, 844 (2007).

[15] T. Akazawa, H. Hidaka, H. Kotegawa, T. C. Kobayashi,T. Fujiwara, E. Yamamoto, Y. Haga, R. Settai, and Y. Ōnuki, J. Phys. Soc. Jpn. 73, 3129 (2004).

[16] S. S. Saxena, P. Agarwal, K. Ahilan, F. M. Grosche, R. K. W. Haselwimmer, M. J. Steiner, E. Pugh, I. R. Walker, S. R. Julian, P. Monthoux, G. G. Lonzarich, A. Huxley, I. Sheikin, D. Braithwaite, and J. Flouquet, Nature 406, 587 (2000).

[17] P. Badica, T. Kondo, and K. Togano, J. Phys. Soc. Jpn. 74, 1014 (2005).

[18] K. Togano, P. Badica, Y.Nakamori, S. Orimo, H.Takeya, and K. Hirata, Phys. Rev. Lett. 93, 247004 (2004).

[19] P. Badica, T. Kondo, T. Kudo, Y. Nakamori, S. Orimo, and K. Togano, Appl. Phys. Lett. 85, 4433 (2004).

[20] H. Takeya, K. Hirata, K. Yamaura, K. Togano, M. El Massalami, R. Rapp, F.A. Chaves, B.Ouladdiaf, Phys. Rev. B 72, 104506 (2005).

[21] J. Chen, L. Jiao, J. L. Zhang, Y. Chen, L. Yang, M. Nicklas, F. Steglich, and H. Q. Yuan, New J. Phys. 15, 053005 (2013).

[22] V. K. Pecharsky, L. L. Miller, K. A. Gschneidner, Phys. Rev. B 58, 497 (1998).

[23] P. K. Biswas, M. R. Lees, A. D. Hillier, R. I. Smith, W. G. Marshall, and D. McK. Paul, Phys. Rev. B 84, 184529 (2011).

[24] T. Klimczuk, F. Ronning, V. Sidorov, R. J. Cava, and J. D. Thompson, Phys. Rev. Lett. 99, 257004 (2007).

[25] Yanpeng Qi, Jiangang Guo, Hechang Lei, Zewen Xiao, Toshio Kamiya, and Hideo Hosono, Phys. Rev. B 89, 024517 (2014).

[26] E. Bauer, G. Rogl, Xing-Qiu Chen, R. T. Khan, H. Michor, G. Hilscher, E. Royanian, K. Kumagai, D. Z. Li, Y. Y. Li, R. Podloucky, and P. Rogl, Phys. Rev. B 82, 064511 (2010).

[27] N. Kase and J. Akimitsu, J. Phys. Soc. Jpn. 78, 044710 (2009).

[28] L. Fang, H. Yang, X. Zhu, G. Mu, Z.-Sheng Wang, L. Shan, C. Ren, and H.-Hu Wen, Phys. Rev. B 79, 144509 (2009).

[29] A. B. Karki, Y. M. Xiong, N. Haldolaarachchige, S. Stadler, I.Vekhter, P. W. Adams, D. P. Young, W. A. Phelan, and J. Y. Chan, Phys. Rev. B 83, 144525 (2011).

[30] C. S. Lue, T. H. Su, H. F. Liu, and B. L. Young, Phys. Rev. B 84, 052509 (2011).

[31] R. P. Singh, A. D. Hillier, B. Mazidian, J. Quintanilla, J. F. Annett, D. M. Paul, G. Balakrishnan, and M. R. Lees, Phys. Rev. Lett. 112, 107002 (2014).

[32] J. A. T. Barker, D. Singh, A. Thamizhavel, A. D. Hillier, M. R. Lees, G. Balakrishnan, D McK. Paul, and R. P. Singh, Phys. Rev. Lett. 115, 267001 (2015).

[33] A. M. Khan, arXiv preprint arXiv:1603.07297 (2016)

[34] M. Nishiyama, Y. Inada, and G.-Q. Zheng, Phys. Rev. Lett. 98, 047002 (2007).

[35] A. B. Karki, Y. M. Xiong, I. Vekhter, D. Browne, P. W. Adams, D. P. Young, K. R. Thomas, J. Y. Chan, H. Kim, and R. Prozorov, Phys. Rev. B 82, 064512 (2010).

[36] C. S. Lue, H. F. Liu, C. N. Kuo, P. S. Shih, J-Y Lin, Y. K. Kuo, M. W. Chu, T-L Hung, and Y. Y. Chen, Superconductor Science and Technology 26, 055011 (2013).

[37] W. L. McMillan, Phys. Rev. 167, 331 (1968).

[38] M. Isobe, A. Masao, and N. Shirakawa, Phys. Rev. B 93, 054519 (2016).

[39] C. Caroli, P. G. de Gennes, and J. Matricon, Phys. Lett. 9, 307(1964).

[40] P. G. de Gennes, *Superconductivity of Metals and Alloys* (W. A. Benjamin, New York, 1966).

[41] G. E. Volovik, JETP Lett. 58, 469 (1993).

[42] K.Kadowaki, and S. B. Woods: Solid state communications 58, 507 (1986).

[43] R. Jin, J. He, S. McCall, C. S. Alexander, F. Drymiotis, and D. Mandrus, Phys. Rev. B 64, 180503 (2001).

[44] A.C. Jacko, J. O. Fjaerestad, and B. J. Powell, Nature Physics 5(6), 422 (2009).

[45] M.Tinkham, *Introduction to Superconductivity* 2nd edn (McGraw - Hill, New York, 1996).

[46] E. Helfand and N. R. Werthamer, Phys. Rev. 147, 288 (1966).

[47] N. R. Werthamer, E. Helfand, and P. C.Hohenberg, Phys. Rev. 147, 295 (1966).

[48] B. S. Chandrasekhar, Appl. Phys. Lett. 1, 7 (1962).

[49] A. M. Clogston: Phys. Rev. Lett. 9, 266 (1962).

[50] K. Maki, Phys. Rev. B 148, 362 (1966).

[51] T. Klimczuk, F. Ronning, V. Sidorov, R. J. Cava, and J. D. Thompson, Phys. Rev. Lett. 99, 257004 (2007)

[52] O. Prakash, A. Thamizhavel, and S. Ramakrishnan, Superconductor Science and Technology 28,15012 (2015).

[53] G. Blatter, *Statistical Mechanics and its Applications* 200.1-4, 341 (1993).